Condon's model on rotatory power and causality - a scientific trifle

Kristensson, Gerhard

Published in:
Festskrift till Staffan Ström

1999

Condon's model on optical rotatory power and causality — a scientific trifle

Gerhard Kristensson
Department of Electromagnetic Theory, Lund University, P.O. Box 118, SE-221 00 Lund, SWEDEN.

Abstract

In this paper some of the consequences of the model for optical activity suggested by Condon are analyzed. The scattering problem is solved for a semi-infinite and a finite homogeneous slab, respectively. Specifically, the non-causal effects of this model are demonstrated. These effects are disturbingly large for many materials and the model has to be discarded as unphysical. The rotation of the polarization plane is shown to agree with the fixed frequency results when the transient part of the solution has died out. Moreover, a new delta sequence that is associated with the Fresnel integrals is analyzed.

1 Prerequisites

The Maxwell equations are the basic equations that model the dynamics of the electromagnetic fields.

$$\begin{cases} \nabla \times \boldsymbol{E}(\boldsymbol{r},t) = -\dfrac{\partial}{\partial t}\boldsymbol{B}(\boldsymbol{r},t) \\ \nabla \times \boldsymbol{H}(\boldsymbol{r},t) = \dfrac{\partial}{\partial t}\boldsymbol{D}(\boldsymbol{r},t) \end{cases} \tag{1.1}$$

These equations, which give the dynamics of the fields, are not complete as a model of the wave propagation in a complex medium. There are in total 12 unknown (4 vector fields), but only 6 equations. The missing 6 equations are given by the constitutive relations, which model the dynamics of the charges in the medium.

The reborn interest in chiral media or, more generally, in bi-isotropic media, has motivated several studies and reviews of the constitutive relations, see, *e.g.*[4, 6, 5, 8, 7]. In a work from 1937 Condon suggests a model for optical rotatory power. Condon [3] suggested the following constitutive relations (see also [7]):

$$\begin{cases} \boldsymbol{D}(\boldsymbol{r},t) = \epsilon\boldsymbol{E}(\boldsymbol{r},t) - \alpha\dfrac{\partial}{\partial t}\boldsymbol{H}(\boldsymbol{r},t) \\ \boldsymbol{B}(\boldsymbol{r},t) = \alpha\dfrac{\partial}{\partial t}\boldsymbol{E}(\boldsymbol{r},t) + \mu\boldsymbol{H}(\boldsymbol{r},t) \end{cases} \tag{1.2}$$

where the magneto-electric effects are modelled by the real constant α. This constant can be both positive and negative, and it has the dimension of reciprocal

acceleration. The constants ϵ and μ are the ordinary permittivity and permeability, respectively, of the medium in the absence of magneto-electric effects.

The aim of this paper is to study the propagation of electromagnetic waves in a medium characterized by the constitutive relations in (1.2). Especially, the violation of causality is investigated and its consequences are discussed.

The Maxwell equations (1.1) and the constitutive relations (1.2) can be combined. The result is

$$\nabla \times \begin{pmatrix} \boldsymbol{E} \\ \eta \boldsymbol{H} \end{pmatrix} = \frac{1}{c} \begin{pmatrix} \mathbf{0} & -\mathbf{I}_3 \\ \mathbf{I}_3 & \mathbf{0} \end{pmatrix} \cdot \frac{\partial}{\partial t} \begin{pmatrix} \boldsymbol{E} \\ \eta \boldsymbol{H} \end{pmatrix} - \alpha \frac{\partial^2}{\partial t^2} \begin{pmatrix} \boldsymbol{E} \\ \eta \boldsymbol{H} \end{pmatrix} \tag{1.3}$$

where $\eta = \sqrt{\mu/\epsilon}$ and $c = 1/\sqrt{\epsilon\mu}$, and $\mathbf{I}_3$ is the three-dimensional identity dyadic[1]. It is, of course, possible to eliminate one of the fields, say the magnetic field $\boldsymbol{H}$, in (1.3), but the order of the partial derivatives then increases to fourth order in time. There are also other reasons, such as energy transport, that are more conveniently expressed as a pair of fields, and, therefore, in this paper, we analyze the equations as they are given in (1.3).

In Section 2 the problem is simplified to a problem with variation in just one spatial coordinate. In Sections 3–4 we address the scattering problem. The discussion on causality and the validity of the Condon's model is found in Section 5. Some technical calculations are presented in a series of appendices.

2 One-dimensional spatial variation

The fields in the previous section were general functions of all spatial coordinates x, y, z. In this section, the fields are restricted to vary only in one coordinate, say the depth z. An alternative, more physically appealing, interpretation is to consider this one-dimensional variation as a result of averaging over the transverse coordinates x and y.

Assume the variation in the fields are one-dimensional, *e.g.*

$$\boldsymbol{E}(\boldsymbol{r}, t) = \boldsymbol{E}_\perp(z, t) + \hat{\boldsymbol{z}} E_z(z, t) = \hat{\boldsymbol{x}} E_x(z, t) + \hat{\boldsymbol{y}} E_y(z, t) + \hat{\boldsymbol{z}} E_z(z, t)$$

where

$$\boldsymbol{E}_\perp(z, t) = \hat{\boldsymbol{z}} \times (\boldsymbol{E}(z, t) \times \hat{\boldsymbol{z}})$$

In a dyadic notation, the rotation then becomes

$$\nabla \times \boldsymbol{E}(\boldsymbol{r}, t) = \mathbf{J} \cdot \frac{\partial}{\partial z} \boldsymbol{E}_\perp(z, t)$$

where the constant two-dimensional dyadic $\mathbf{J}$ is defined as

$$\mathbf{J} = \hat{\boldsymbol{z}} \times \mathbf{I}_2$$

[1] Throughout this paper a dyadic notation is adopted and all dyadics are typed in roman boldface and vectors in italic boldface. Furthermore, no distinction is made between vectors and their representation as column vectors of cartesian coordinates in this paper.

where $\mathbf{I}_2$ is the two-dimensional identity dyadic in the x-y-plane. This dyadic represents a rotation of $\pi/2$ in the x-y-plane. Notice that

$$\mathbf{J}\cdot\mathbf{J}^t = -\mathbf{J}\cdot\mathbf{J} = \mathbf{I}_2$$

where the superscript $(^t)$ denotes the transpose of the dyadic.

The transverse components of (1.3) can then be written as

$$\frac{\partial}{\partial z}\begin{pmatrix}\mathbf{J}\cdot\boldsymbol{E}_\perp\\ \eta\mathbf{J}\cdot\boldsymbol{H}_\perp\end{pmatrix} = \frac{1}{c}\frac{\partial}{\partial t}\begin{pmatrix}\mathbf{0} & -\mathbf{I}_2\\ \mathbf{I}_2 & \mathbf{0}\end{pmatrix}\cdot\begin{pmatrix}\boldsymbol{E}_\perp\\ \eta\boldsymbol{H}_\perp\end{pmatrix} - \alpha\frac{\partial^2}{\partial t^2}\begin{pmatrix}\boldsymbol{E}_\perp\\ \eta\boldsymbol{H}_\perp\end{pmatrix}$$

The z-components of (1.3) are

$$\begin{cases} c\alpha\dfrac{\partial^2 E_z}{\partial t^2} + \eta\dfrac{\partial H_z}{\partial t} = 0\\ c\alpha\eta\dfrac{\partial^2 H_z}{\partial t^2} - \dfrac{\partial E_z}{\partial t} = 0\end{cases}$$

The general solutions to these equations are

$$\begin{cases} E_z(z,t) = A_1(z)\sin\dfrac{t}{c\alpha} + A_2(z)\cos\dfrac{t}{c\alpha} + A_3(z)\\ H_z(z,t) = B_1(z)\sin\dfrac{t}{c\alpha} + B_2(z)\cos\dfrac{t}{c\alpha} + B_3(z)\end{cases}$$

If all fields are assumed to vanish as $t\to-\infty$, all constants of integrations are zero and

$$\begin{cases} E_z(z,t) = 0\\ H_z(z,t) = 0\end{cases}$$

and all fields, $\boldsymbol{E}$, $\boldsymbol{H}$, $\boldsymbol{D}$, and $\boldsymbol{B}$ are transverse by the use of the constitutive relations (1.2).

It is appropriate to rewrite the equation of the transverse components as

$$\frac{\partial}{\partial z}\begin{pmatrix}\boldsymbol{E}_\perp\\ \eta\mathbf{J}\cdot\boldsymbol{H}_\perp\end{pmatrix} = \frac{1}{c}\frac{\partial}{\partial t}\begin{pmatrix}\mathbf{0} & \mathbf{I}_2\\ \mathbf{I}_2 & \mathbf{0}\end{pmatrix}\cdot\begin{pmatrix}\boldsymbol{E}_\perp\\ \eta\mathbf{J}\cdot\boldsymbol{H}_\perp\end{pmatrix} + \alpha\frac{\partial^2}{\partial t^2}\begin{pmatrix}\mathbf{J} & \mathbf{0}\\ \mathbf{0} & \mathbf{J}\end{pmatrix}\cdot\begin{pmatrix}\boldsymbol{E}_\perp\\ \eta\mathbf{J}\cdot\boldsymbol{H}_\perp\end{pmatrix}$$

To avoid cumbersome notation we define the four-dimensional vector $\boldsymbol{u}(z,t)$

$$\boldsymbol{u}(z,t) = \begin{pmatrix}\boldsymbol{E}_\perp(z,t)\\ \eta\mathbf{J}\cdot\boldsymbol{H}_\perp(z,t)\end{pmatrix} \tag{2.1}$$

and the two four-dimensional dyadics $\mathbf{A}$ and $\mathbf{B}$

$$\mathbf{A} = \begin{pmatrix}\mathbf{J} & \mathbf{0}\\ \mathbf{0} & \mathbf{J}\end{pmatrix}, \qquad \mathbf{B} = \begin{pmatrix}\mathbf{0} & \mathbf{I}_2\\ \mathbf{I}_2 & \mathbf{0}\end{pmatrix}$$

Notice that $\mathbf{A}$ and $\mathbf{B}$ commute and

$$\mathbf{A}\cdot\mathbf{A} = -\mathbf{I}_4, \qquad \mathbf{B}\cdot\mathbf{B} = \mathbf{I}_4$$

where $\mathbf{I}_4$ denotes the four-dimensional identity dyadic.

The fundamental equation is therefore

$$\frac{\partial}{\partial z}\boldsymbol{u} = \alpha\mathbf{A}\cdot\frac{\partial^2}{\partial t^2}\boldsymbol{u} + \frac{1}{c}\mathbf{B}\cdot\frac{\partial}{\partial t}\boldsymbol{u} \tag{2.2}$$

This equation shows resemblance with the ordinary parabolic equations if the time variable t and spatial variable z are interchanged.

2.1 Wave splitting

The Poynting vector can also expressed in terms of the vector $\boldsymbol{u}$.

$$\boldsymbol{P}(z,t) = \boldsymbol{E}(z,t)\times\boldsymbol{H}(z,t) = -\left(\boldsymbol{E}_\perp\cdot\mathbf{J}\cdot\boldsymbol{H}_\perp\right)\hat{\boldsymbol{z}} = -\frac{\hat{\boldsymbol{z}}}{2\eta}\boldsymbol{u}\cdot\mathbf{B}\cdot\boldsymbol{u}$$

by standard dyadic operations. The vector $\boldsymbol{u}$ is decomposed as

$$\boldsymbol{u}(z,t) = \begin{pmatrix}\boldsymbol{u}_+(z,t)+\boldsymbol{u}_-(z,t)\\ \boldsymbol{u}_-(z,t)-\boldsymbol{u}_+(z,t)\end{pmatrix} = \begin{pmatrix}\mathbf{I}_2 & \mathbf{I}_2\\ -\mathbf{I}_2 & \mathbf{I}_2\end{pmatrix}\cdot\begin{pmatrix}\boldsymbol{u}_+(z,t)\\ \boldsymbol{u}_-(z,t)\end{pmatrix} \tag{2.3}$$

where the transverse two-dimensional vectors $\boldsymbol{u}_+(z,t)$ and $\boldsymbol{u}_-(z,t)$ are defined as

$$\begin{pmatrix}\boldsymbol{u}_+(z,t)\\ \boldsymbol{u}_-(z,t)\end{pmatrix} = \frac{1}{2}\begin{pmatrix}\mathbf{I}_2 & -\mathbf{I}_2\\ \mathbf{I}_2 & \mathbf{I}_2\end{pmatrix}\cdot\begin{pmatrix}\boldsymbol{E}_\perp(z,t)\\ \eta\mathbf{J}\cdot\boldsymbol{H}_\perp(z,t)\end{pmatrix} = \frac{1}{2}\begin{pmatrix}\mathbf{I}_2 & -\mathbf{I}_2\\ \mathbf{I}_2 & \mathbf{I}_2\end{pmatrix}\cdot\boldsymbol{u}(z,t) \tag{2.4}$$

The fields $\boldsymbol{u}_+$ and $\boldsymbol{u}_-$ are called the split fields due to the fact that the Poynting vector is

$$\boldsymbol{P}(z,t) = \frac{\hat{\boldsymbol{z}}}{\eta}\left[|\boldsymbol{u}_+(z,t)|^2 - |\boldsymbol{u}_-(z,t)|^2\right] \tag{2.5}$$

The two fields $\boldsymbol{u}_+$ and $\boldsymbol{u}_-$ therefore give the contributions of the power sent in the positive and negative direction, respectively. The original fields, $\boldsymbol{E}_\perp$ and $\boldsymbol{H}_\perp$, are easily retrieved from (2.3), see also (2.1). We have

$$\begin{pmatrix}\boldsymbol{E}_\perp(z,t)\\ \boldsymbol{H}_\perp(z,t)\end{pmatrix} = \begin{pmatrix}\mathbf{I}_2 & \mathbf{I}_2\\ \frac{1}{\eta}\mathbf{J} & -\frac{1}{\eta}\mathbf{J}\end{pmatrix}\cdot\begin{pmatrix}\boldsymbol{u}_+(z,t)\\ \boldsymbol{u}_-(z,t)\end{pmatrix}$$

Continuity of the tangential fields, $\boldsymbol{E}_\perp$ and $\boldsymbol{H}_\perp$, implies that the fields

$$\boldsymbol{u}_+ + \boldsymbol{u}_- \quad\text{and}\quad \left(\boldsymbol{u}_+ - \boldsymbol{u}_-\right)/\eta$$

are continuous.

The transformation of dependent variables given by (2.4) implies that the original PDE (2.2) is equivalent to

$$\frac{\partial\boldsymbol{u}_\pm(z,t)}{\partial z} \pm \frac{1}{c}\frac{\partial\boldsymbol{u}_\pm(z,t)}{\partial t} = \alpha\mathbf{J}\cdot\frac{\partial^2\boldsymbol{u}_\pm(z,t)}{\partial t^2}$$

and we see that the transformation in (2.4) decouples the four-dimensional system (2.2) into a two-dimensional system. This system can be reduced further by a simple change of the independent variables. We get

$$\frac{d\boldsymbol{u}_\pm(z,t\pm z/c)}{dz} = \alpha\mathbf{J}\cdot\frac{\partial^2\boldsymbol{u}_\pm(z,t\pm z/c)}{\partial t^2} \tag{2.6}$$

2.2 Boundary value problem

The following boundary value problem is pertinent for the analysis in this paper:

$$\begin{cases} \dfrac{d\boldsymbol{u}_\pm(z,t\pm z/c)}{dz} = \alpha\mathbf{J}\cdot\dfrac{\partial^2\boldsymbol{u}_\pm(z,t\pm z/c)}{\partial t^2}, & z\geq 0 \qquad t\in\mathbb{R} \\ \boldsymbol{u}_\pm(0,t) = \boldsymbol{u}_0(t) \end{cases}$$

This problem is solved in Appendix A, see (A.1).

$$\boldsymbol{u}_\pm(z,t) = \left(\mathbf{f}(\alpha z,\cdot)*\boldsymbol{u}_0(\cdot)\right)(t\mp z/c) + \left(\mathbf{g}(\alpha z,\cdot)*\boldsymbol{u}_0(\cdot)\right)(t\mp z/c) \tag{2.7}$$

where we have introduced the following dyadic-valued functions

$$\begin{cases} \mathbf{f}(a,t) = \dfrac{1}{\sqrt{4\pi|a|}}\cos\left(t^2/4|a|-\pi/4\right)\mathbf{I}_2 \\ \mathbf{g}(a,t) = -\dfrac{\operatorname{sign} a}{\sqrt{4\pi|a|}}\cos\left(t^2/4|a|+\pi/4\right)\mathbf{J} \end{cases}$$

The temporal convolution of a dyadic-valued function $\mathbf{f}_1$ and a vector-valued function $\boldsymbol{f}_2$ is defined as

$$\left(\mathbf{f}_1(z,\cdot)*\boldsymbol{f}_2(\cdot)\right)(\tau) = \int_{-\infty}^{\infty}\mathbf{f}_1(z,\tau-\tau')\cdot\boldsymbol{f}_2(\tau')\,d\tau'$$

The solution of the scattering inside the material, (2.7), is non-causal, due to the fact that the temporal integration in the convolutions extends over the entire real axis, and not just to the positive real axis. We illustrate this situation in the following two sections, but first we note that the boundary conditions are met by the limits of the dyadic-valued functions $\mathbf{f}$ and $\mathbf{g}$. We have the limit values, see (D.3).

$$\begin{cases} \lim\limits_{a\to 0}\mathbf{f}(a,t) = \mathbf{I}_2\delta(t) \\ \lim\limits_{a\to 0}\mathbf{g}(a,t) = \mathbf{0} \end{cases}$$

3 Scattering problem—semi-infinite slab

We illustrate the effects of the lack of causality by solving scattering by a semi-infinite slab. The geometry is depicted in Figure 1. The left half-space, $z<0$, is assumed to be an isotropic medium with permittivity ϵ_1 and permeability μ_1, and the right half-space, $z>0$, is a bi-isotropic material modelled by Condon's model, (1.2), and parameterized by ϵ, μ, and α.

Assume there are no sources in the region $z>0$. The only sources are located in the left half-space, $z<0$. The general solution to the left of the scatterer, $z<0$, is assumed to be, see (2.3) and (2.6) with $\alpha=0$

$$\boldsymbol{u}(z,t) = \begin{pmatrix} \boldsymbol{E}_i(t-z/c_1)+\boldsymbol{E}_r(t+z/c_1) \\ \boldsymbol{E}_r(t+z/c_1)-\boldsymbol{E}_i(t-z/c_1) \end{pmatrix} \qquad z<0$$

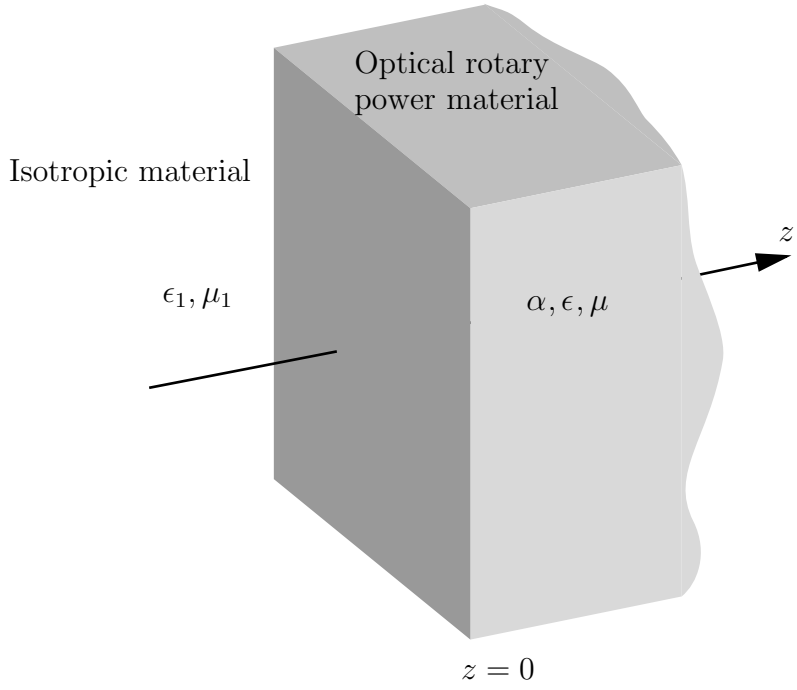

Figure 1: The geometry of the semi-infinite slab.

where $c_1 = 1/\sqrt{\epsilon_1 \mu_1}$. The vector fields $\boldsymbol{E}_i(t)$ and $\boldsymbol{E}_r(t)$ are the incident and the reflected fields at $z = 0$, respectively, transporting power to the right and to the left, respectively.

The solution to the left of the scatterer at $z = 0^-$ is

$$\boldsymbol{u}(0^-, t) = \begin{pmatrix} \boldsymbol{E}_i(t) + \boldsymbol{E}_r(t) \\ \boldsymbol{E}_r(t) - \boldsymbol{E}_i(t) \end{pmatrix}$$

and inside the slab $\boldsymbol{u}_-(z, t) = \boldsymbol{0}$ for all $z > 0$, due to the fact that there are no sources in the half-space $z > 0$. Therefore, the appropriate boundary conditions at the interface $z = 0$ are

$$\begin{cases} \boldsymbol{u}_+(0^+, t) = \boldsymbol{E}_i(t) + \boldsymbol{E}_r(t) \\ \boldsymbol{u}_+(0^+, t)/\eta = \left(\boldsymbol{E}_i(t) - \boldsymbol{E}_r(t)\right)/\eta_1 \end{cases}$$

where $\eta_1 = \sqrt{\mu_1/\epsilon_1}$. Elimination of the field $\boldsymbol{E}_r(t)$ gives

$$\boldsymbol{u}_+(0^+, t) = \frac{2\eta}{\eta + \eta_1} \boldsymbol{E}_i(t) = t_0^+ \boldsymbol{E}_i(t)$$

where we have introduced the transmission coefficient for transmission to the right

$$t_0^+ = \frac{2\eta}{\eta + \eta_1}$$

Moreover, elimination of the field $\boldsymbol{u}_+(0^+, t)$ gives the reflected field $\boldsymbol{E}_r(t)$

$$\boldsymbol{E}_r(t) = \frac{\eta - \eta_1}{\eta + \eta_1} \boldsymbol{E}_i(t) = r_0^+ \boldsymbol{E}_i(t) \tag{3.1}$$

Here the reflection coefficient of the slab from the left is

$$r_0^+ = \frac{\eta - \eta_1}{\eta + \eta_1}$$

and reflection occurs only at the interface. Note that this reflected field is a causal response of the incident field and independent of the parameter α.

The pertinent problem for the semi-infinite medium is:

$$\begin{cases} \dfrac{d\boldsymbol{u}_+(z,t+z/c)}{dz} = \alpha \mathbf{J} \cdot \dfrac{\partial^2 \boldsymbol{u}_+(z,t+z/c)}{\partial t^2}, & z \geq 0 \qquad t \in \mathbb{R} \\ \boldsymbol{u}_+(0,t) = t_0^+ \boldsymbol{E}_i(t) \end{cases}$$

The solution to the problem is, see (2.7)

$$\boldsymbol{u}_+(z,t) = t_0^+ \left[(\mathbf{f}(\alpha z,\cdot) * \boldsymbol{E}_i(\cdot))(t-z/c) + (\mathbf{g}(\alpha z,\cdot) * \boldsymbol{E}_i(\cdot))(t-z/c) \right], \qquad z > 0$$

Note that the field inside the medium goes to zero as $|t| \to \infty$, if $\boldsymbol{E}_i \in L_1(\mathbb{R})^2$ as seen from (C.2) in Appendix C. Again, notice that the transmitted field in the slab is non-causal.

3.1 Example

We quantify the effects of the lack of causality by a specific example. Let

$$\boldsymbol{E}_i(t) = \hat{\boldsymbol{x}} H(t) \sin \omega_0 t$$

where $H(t)$ is the Heaviside step function ($H(t) = 1$, $t > 0$, zero otherwise) and $\omega_0 > 0$.

It is convenient to introduce dimensionless variables. To this end, define the two dimensionless parameters

$$\begin{cases} \tau = \omega_0 t \\ \zeta = z\omega_0/c \end{cases}$$

The incident field is then

$$\boldsymbol{E}_i(\tau) = \hat{\boldsymbol{x}} H(\tau) \sin \tau$$

The reflected field is, see (3.1)

$$\boldsymbol{E}_r(\tau) = \hat{\boldsymbol{x}} H(\tau) r_0^+ \sin \tau$$

and the field inside the medium can be calculated using (C.1) in Appendix C. The result is, $\zeta > 0$

$$\boldsymbol{E}(\zeta,\tau) = t_0^+ H(\tau-\zeta) \sin(\tau-\zeta) (\hat{\boldsymbol{x}} \cos\chi + \hat{\boldsymbol{y}} \sin\chi) + \boldsymbol{E}_{\text{transient}}(\zeta,\tau) \tag{3.2}$$

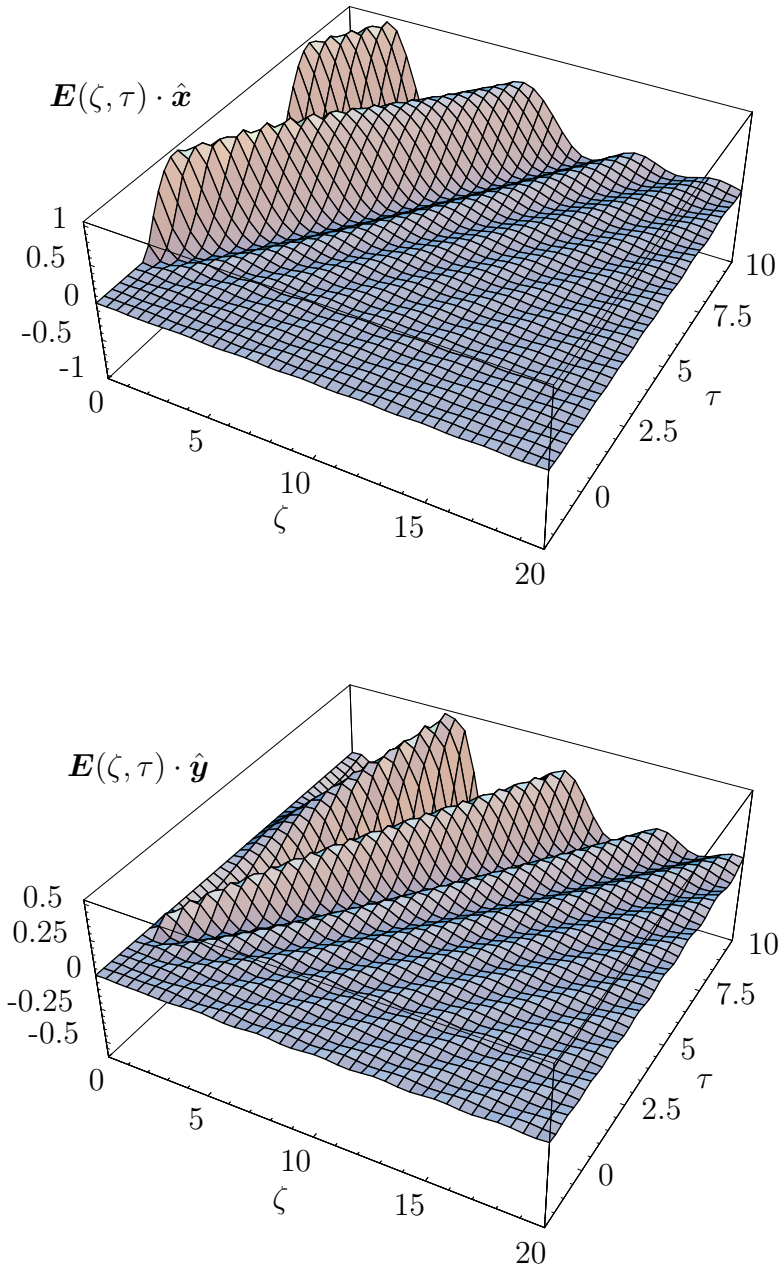

Figure 2: The fields $\boldsymbol{E}(\zeta,\tau)\cdot\hat{\boldsymbol{x}}$ and $\boldsymbol{E}(\zeta,\tau)\cdot\hat{\boldsymbol{y}}$ for $\omega_0\alpha c = .1\ \mathrm{m}^{-1}$.

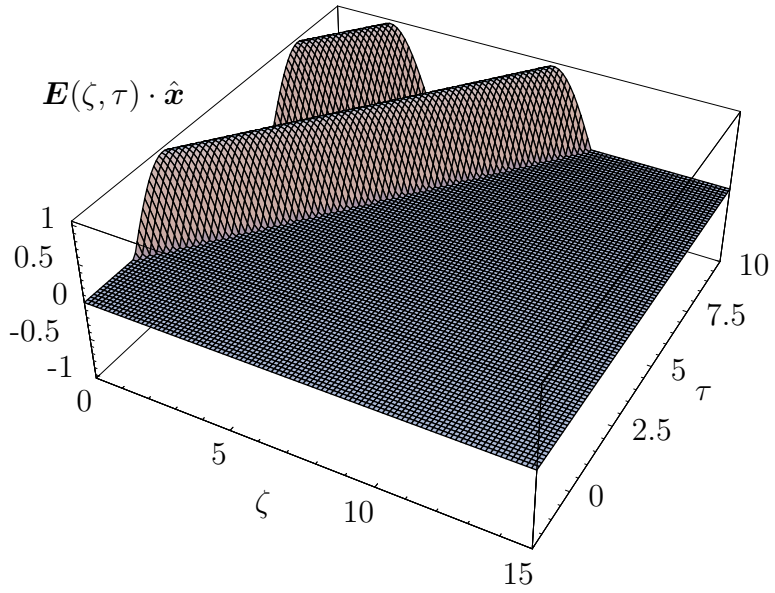

Figure 3: The field $\boldsymbol{E}(\zeta,\tau)\cdot\hat{\boldsymbol{x}}$ for $\omega_0\alpha c = 1.\,10^{-6}$ m^{-1}.

The angle of rotation of the polarization of the field as $\tau\to\infty$ is

$$\chi = \chi(\zeta) = -\omega_0^2\alpha z = -\omega_0\alpha c\zeta$$

which agrees with the result of fixed frequency analysis.[2] The transient field is ($\zeta > 0$)

$$\begin{aligned}
&\boldsymbol{E}_{\text{transient}}(\zeta,\tau)\\
&\quad= \frac{t_0^+}{4}\Big\{\hat{\boldsymbol{x}}\sin(\tau-\zeta)\Big\{\cos\chi\,[C(\gamma_+)+C(\gamma_-)+S(\gamma_+)+S(\gamma_-)-2\,\text{sign}\,(\tau-\zeta)]\\
&\qquad\qquad+\sin|\chi|\,[S(\gamma_+)+S(\gamma_-)-C(\gamma_+)-C(\gamma_-)]\Big\}\\
&\qquad+\hat{\boldsymbol{x}}\cos(\tau-\zeta)\Big\{[\cos\chi+\sin|\chi|]\,[C(\gamma_+)-C(\gamma_-)]\\
&\qquad\qquad-[\cos\chi-\sin|\chi|]\,[S(\gamma_+)-S(\gamma_-)]\Big\}\\
&\qquad+\hat{\boldsymbol{y}}\sin(\tau-\zeta)\Big\{\text{sign}\,(\alpha)\cos\chi\,[S(\gamma_+)+S(\gamma_-)-C(\gamma_+)-C(\gamma_-)]\\
&\qquad\qquad+\sin\chi\,[C(\gamma_+)+C(\gamma_-)+S(\gamma_+)+S(\gamma_-)-2\,\text{sign}\,(\tau-\zeta)]\Big\}\\
&\qquad+\hat{\boldsymbol{y}}\,\text{sign}\,(\alpha)\cos(\tau-\zeta)\Big\{[\cos\chi-\sin|\chi|]\,[C(\gamma_+)-C(\gamma_-)]\\
&\qquad\qquad+[\cos\chi+\sin|\chi|]\,[S(\gamma_+)-S(\gamma_-)]\Big\}\Big\}
\end{aligned}$$

[2]The relation between the notation of Ref. [8] and this paper is $\kappa = \alpha\omega_0/\sqrt{\epsilon_0\mu_0}$.

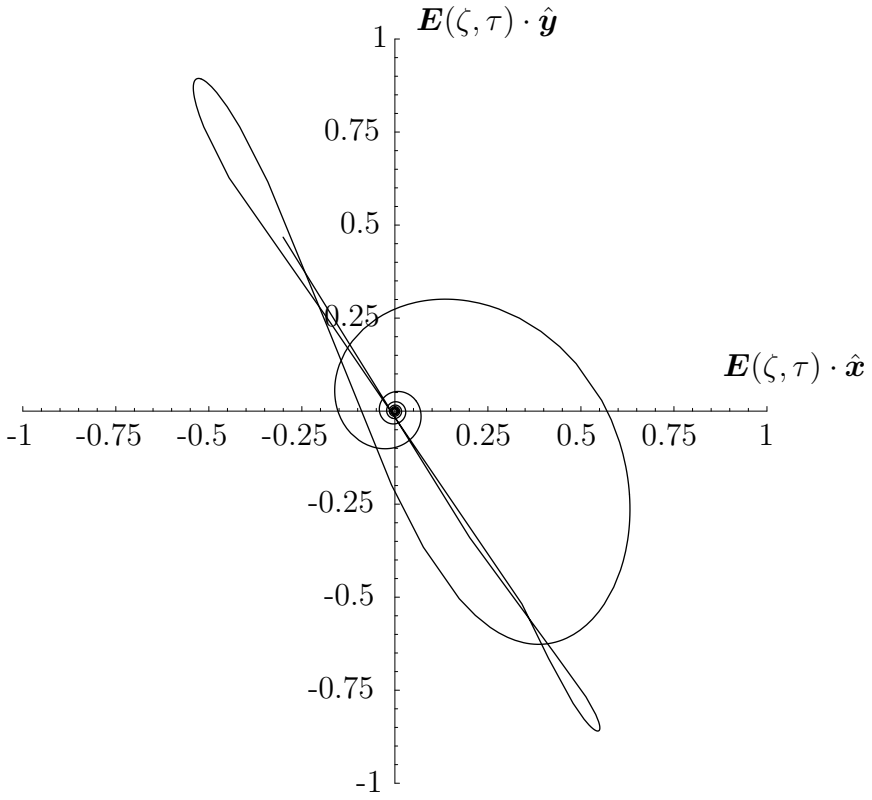

Figure 4: The field polarization of the field at $\zeta = 10$ for $\omega_0 \alpha c = .1\ \mathrm{m}^{-1}$. Time τ is the parameter along the curve.

where

$$\gamma_\pm = \sqrt{\frac{8\,|\alpha z|}{\pi}}\left(\frac{t - z/c}{4|\alpha z|} \pm \frac{\omega_0}{2}\right) = \sqrt{\frac{2\,|\chi|}{\pi}}\left(\frac{\tau - \zeta}{2|\chi|} \pm 1\right)$$

and the Fresnel integrals $C(z)$ and $S(z)$ are defined in Appendix C. The first term in (3.2) is causal due to the Heaviside function, but $\boldsymbol{E}_{\text{transient}}(\zeta,\tau)$ contains non-causal terms. The field $\boldsymbol{E}_{\text{transient}} \to 0$ as $\tau \to \pm\infty$.

The result of this example is depicted in Figures 2–4. We observe that for small values of α, *e.g.*$\omega_0 \alpha c = 1 \cdot 10^{-6}\ \mathrm{m}^{-1}$, the effects of the non-causality are negligible.

4 Scattering problem—finite slab

In this section we analyze the finite slab problem depicted in Figure 5. The solution of this scattering problem relies on the solution obtained in Section 3. The left and the right half-spaces, $z < 0$ and $z > L$, respectively, are assumed to be isotropic materials, parameterized by the permittivity and permeability ϵ_1, μ_1, ϵ_2, and μ_2, respectively. The slab, $0 < z < L$, is a bi-isotropic material modelled by Condon's model, (1.2), and parameterized by ϵ, μ, and α.

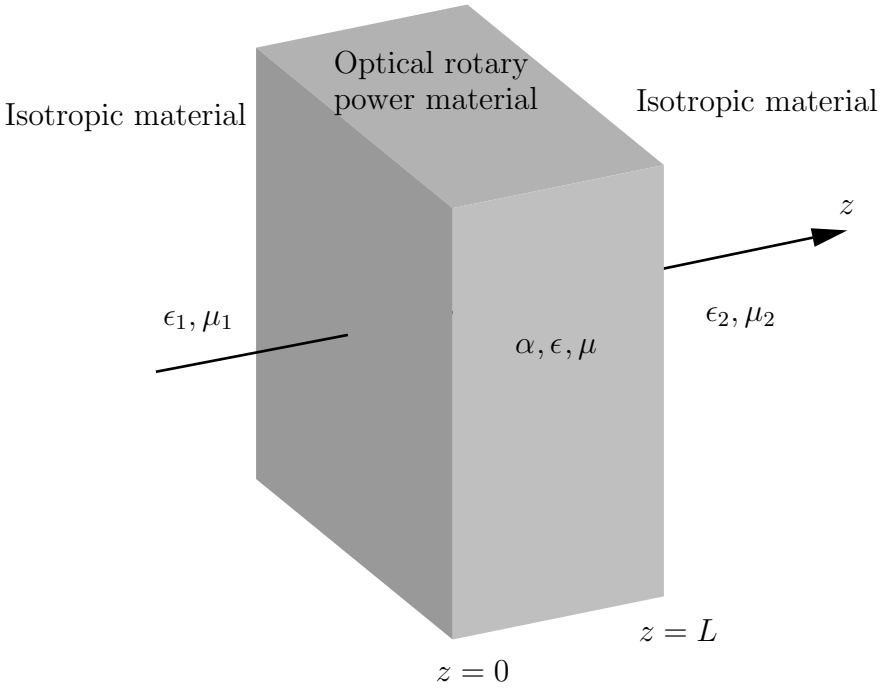

Figure 5: The geometry of the finite slab.

Assume there are no sources in the region $z > L$. The only sources are located in the left half-space, $z < 0$. The general solution to the left of the scatterer $z < 0$, but to the right of the sources is assumed to be, see (2.3) and (2.6) with $\alpha = 0$

$$\boldsymbol{u}(z,t) = \begin{pmatrix} \boldsymbol{E}_i(t - z/c_1) + \boldsymbol{E}_r(t + z/c_1) \\ \boldsymbol{E}_r(t + z/c_1) - \boldsymbol{E}_i(t - z/c_1) \end{pmatrix} \qquad z < 0$$

where $c_1 = 1/\sqrt{\epsilon_1\mu_1}$. To the right of the scatterer $z > L$, we have

$$\boldsymbol{u}(z,t) = \begin{pmatrix} \boldsymbol{E}_t(t - (z-L)/c_2) \\ -\boldsymbol{E}_t(t - (z-L)/c_2) \end{pmatrix} \qquad z > L$$

where $c_2 = 1/\sqrt{\epsilon_2\mu_2}$.

The solution to the left of the scatterer at $z = 0^-$ is

$$\boldsymbol{u}(0^-,t) = \begin{pmatrix} \boldsymbol{E}_i(t) + \boldsymbol{E}_r(t) \\ \boldsymbol{E}_r(t) - \boldsymbol{E}_i(t) \end{pmatrix}$$

and to the right of the scatterer at $z = L^+$ is

$$\boldsymbol{u}(L^+,t) = \begin{pmatrix} \boldsymbol{E}_t(t) \\ -\boldsymbol{E}_t(t) \end{pmatrix}$$

The tangential electric field $\boldsymbol{E}_\perp$ and the tangential magnetic field $\boldsymbol{H}_\perp$ are continuous over the boundaries $z = 0, L$. Apply the wave splitting of (2.3)

$$\boldsymbol{u}(z,t) = \begin{pmatrix} \boldsymbol{u}_+(z,t) + \boldsymbol{u}_-(z,t) \\ \boldsymbol{u}_-(z,t) - \boldsymbol{u}_+(z,t) \end{pmatrix}$$

and we get

$$\begin{cases} \boldsymbol{u}_+(0^+,t)+\boldsymbol{u}_-(0^+,t)=\boldsymbol{E}_i(t)+\boldsymbol{E}_r(t) \\ \dfrac{1}{\eta}\left(\boldsymbol{u}_+(0^+,t)-\boldsymbol{u}_-(0^+,t)\right)=\dfrac{1}{\eta_1}\left(\boldsymbol{E}_i(t)-\boldsymbol{E}_r(t)\right) \\ \boldsymbol{u}_+(L^-,t)+\boldsymbol{u}_-(L^-,t)=\boldsymbol{E}_t(t) \\ \dfrac{1}{\eta}\left(\boldsymbol{u}_+(L^-,t)-\boldsymbol{u}_-(L^-,t)\right)=\dfrac{1}{\eta_2}\boldsymbol{E}_t(t) \end{cases}$$

where $\eta_1=\sqrt{\mu_1/\epsilon_1}$, and $\eta_2=\sqrt{\mu_2/\epsilon_2}$. Rearranging the terms gives

$$\begin{cases} \dfrac{1}{2}\left[\boldsymbol{u}_+(0^+,t)\left(1+\dfrac{\eta_1}{\eta}\right)+\boldsymbol{u}_-(0^+,t)\left(1-\dfrac{\eta_1}{\eta}\right)\right]=\boldsymbol{E}_i(t) \\ \dfrac{1}{2}\left[\boldsymbol{u}_+(L^-,t)\left(1-\dfrac{\eta_2}{\eta}\right)+\boldsymbol{u}_-(L^-,t)\left(1+\dfrac{\eta_2}{\eta}\right)\right]=\boldsymbol{0} \end{cases} \tag{4.1}$$

and

$$\begin{cases} \boldsymbol{E}_r(t)=\dfrac{1}{2}\left[\boldsymbol{u}_+(0^+,t)\left(1-\dfrac{\eta_1}{\eta}\right)+\boldsymbol{u}_-(0^+,t)\left(1+\dfrac{\eta_1}{\eta}\right)\right] \\ \boldsymbol{E}_t(t)=\dfrac{1}{2}\left[\boldsymbol{u}_+(L^-,t)\left(1+\dfrac{\eta_2}{\eta}\right)+\boldsymbol{u}_-(L^-,t)\left(1-\dfrac{\eta_2}{\eta}\right)\right] \end{cases} \tag{4.2}$$

The pertinent problem for the finite slab is, see (2.6) and (4.1)

$$\begin{cases} \dfrac{d\boldsymbol{u}_\pm(z,t\pm z/c)}{dz}=\alpha\mathbf{J}\cdot\dfrac{\partial^2\boldsymbol{u}_\pm(z,t\pm z/c)}{\partial t^2}, \quad 0<z<L \\ \boldsymbol{u}_+(0^+,t)-r_0^-\boldsymbol{u}_-(0^+,t)=t_0^+\boldsymbol{E}_i(t) \\ r_L^+\boldsymbol{u}_+(L^-,t)-\boldsymbol{u}_-(L^-,t)=\boldsymbol{0} \end{cases} \qquad t\in\mathbb{R} \tag{4.3}$$

where

$$r_0^-=\frac{\eta_1-\eta}{\eta_1+\eta} \qquad r_L^+=\frac{\eta_2-\eta}{\eta_2+\eta} \qquad t_0^+=\frac{2\eta}{\eta_1+\eta}$$

The reflection coefficient r_0^- is the reflection coefficient at the left edge for reflection from the right and r_L^+ is the corresponding quantity at the right edge from the left. Moreover, t_0^+ is the transmission coefficients at the left edge for transmission to the right. Note that the two fields $\boldsymbol{u}_\pm$ do not couple through the PDE, but they do couple through the boundary conditions.

The solution to this boundary value problem is given in Appendix B, see (B.2) $(0<z<L)$

$$\begin{pmatrix} \boldsymbol{u}_+(z,t) \\ \boldsymbol{u}_-(z,t) \end{pmatrix} = t_0^+\sum_{n=0}^{\infty}\left(r_0^-\right)^n\left(r_L^+\right)^n\left[\mathbf{f}(\alpha z,\cdot)+\mathbf{g}(\alpha z,\cdot)\right]*\begin{pmatrix} \boldsymbol{E}_i(\cdot-z/c-2nL/c) \\ r_L^+\boldsymbol{E}_i(\cdot+z/c-2(n+1)L/c) \end{pmatrix}(t)$$

where the dyadics $\mathbf{f}(a,t)$ and $\mathbf{g}(a,t)$ are defined in Section 2.2 above. Especially, at $z = 0^+$ and $z = L^-$ we get

$$\begin{pmatrix} \boldsymbol{u}_+(0^+,t) \\ \boldsymbol{u}_-(0^+,t) \end{pmatrix} = t_0^+ \sum_{n=0}^{\infty} \left(r_0^-\right)^n \left(r_L^+\right)^n \begin{pmatrix} \boldsymbol{E}_i(t-2nL/c) \\ r_L^+ \boldsymbol{E}_i(t-2(n+1)L/c) \end{pmatrix}$$

and

$$\begin{pmatrix} \boldsymbol{u}_+(L^-,t) \\ \boldsymbol{u}_-(L^-,t) \end{pmatrix} = t_0^+ \sum_{n=0}^{\infty} \left(r_0^-\right)^n \left(r_L^+\right)^n \left[\mathbf{f}(\alpha L,\cdot) + \mathbf{g}(\alpha L,\cdot)\right] * \begin{pmatrix} \boldsymbol{E}_i(\cdot-(2n+1)L/c) \\ r_L^+ \boldsymbol{E}_i(\cdot-(2n+1)L/c) \end{pmatrix}(t)$$

The reflected field $\boldsymbol{E}_r(t)$ and the transmitted field $\boldsymbol{E}_t(t)$ can now be calculated from (4.2). The result is

$$\begin{cases} \boldsymbol{E}_r(t) = r_0^+ \boldsymbol{E}_i(t) + t_0^- t_0^+ \sum_{n=1}^{\infty} \left(r_0^-\right)^{n-1} \left(r_L^+\right)^n \boldsymbol{E}_i(t-2nL/c) \\ \boldsymbol{E}_t(t) = t_0^+ t_L^+ \sum_{n=0}^{\infty} \left(r_0^-\right)^n \left(r_L^+\right)^n \left[\mathbf{f}(\alpha L,\cdot) + \mathbf{g}(\alpha L,\cdot)\right] * \boldsymbol{E}_i(\cdot-(2n+1)L/c)(t) \end{cases} \tag{4.4}$$

where

$$r_0^+ = \frac{\eta - \eta_1}{\eta_1 + \eta} \qquad t_0^- = \frac{2\eta_1}{\eta_1 + \eta} \qquad t_L^+ = \frac{2\eta_2}{\eta_2 + \eta}$$

r_0^+ is the reflection coefficients at the left edge for reflection from the left, t_0^- is the transmission coefficients at the left edge for transmission to the left and t_L^+ is the transmission coefficient at the right edge for transmission to the right. Notice that the reflected field is independent of the parameter α. Furthermore, the reflected field is causal. The transmitted field is not causal.

From (4.4) the reflection kernel $\mathbf{R}(t)$ and the transmission kernel $\mathbf{T}(t)$ can be extracted. The result is

$$\begin{cases} \boldsymbol{E}_r(t) = (\mathbf{R} * \boldsymbol{E}_i)(t) \\ \boldsymbol{E}_t(t) = (\mathbf{T} * \boldsymbol{E}_i)(t) \end{cases}$$

where

$$\begin{cases} \mathbf{R}(t) = r_0^+ \delta(t) \mathbf{I}_2 + t_0^- t_0^+ \sum_{n=1}^{\infty} \left(r_0^+\right)^{n-1} \left(r_L^+\right)^n \delta(t-2nL/c) \mathbf{I}_2 \\ \mathbf{T}(t) = t_0^+ t_L^+ \sum_{n=0}^{\infty} \left(r_0^-\right)^n \left(r_L^+\right)^n \left[\mathbf{f}(\alpha L, t-(2n+1)L/c) + \mathbf{g}(\alpha L, t-(2n+1)L/c)\right] \end{cases}$$

The transmission kernel is not causal, but the reflection kernel is, due to the delta functions that are zero for $t < 0$, *i.e.*$\mathbf{R}(t) = 0$ for $t < 0$. The sum in the transmission kernel $\mathbf{T}$ is always infinite for a fixed value of t, but it remains finite for the reflection kernel $\mathbf{R}$.

4.1 Example

We illustrate the scattering problem in this section by a specific example. Let

$$\boldsymbol{E}_i(t) = \hat{\boldsymbol{x}} H(t) \sin \omega_0 t$$

From (4.4) the reflected field is

$$\begin{aligned}\boldsymbol{E}_r(t) =& \hat{\boldsymbol{x}} \Bigg\{ H(t) r_0^+ \sin \omega_0 t \\ &+ t_0^- t_0^+ \sum_{n=1}^{\infty} \left(r_0^-\right)^{n-1} \left(r_L^+\right)^n H(t - 2nL/c) r_0^+ \sin \omega_0 (t - 2nL/c) \Bigg\}\end{aligned}$$

and the transmitted field can be calculated using (C.1) in Appendix C.

$$\begin{aligned}\boldsymbol{E}_t(t) =& \text{ transient } + t_0^+ t_L^+ \left[\hat{\boldsymbol{x}} \cos\chi + \hat{\boldsymbol{y}} \sin\chi\right] \\ &\cdot \sum_{n=0}^{\infty} \left(r_0^-\right)^n \left(r_L^+\right)^n H(\omega_0 t - (2n+1)L/c) \sin(\omega_0 t - (2n+1)L/c)\end{aligned}$$

The angle of rotation of the polarization of the field as $t \to \infty$ is

$$\chi = -\omega_0^2 \alpha L$$

which agrees with the result of fixed frequency analysis.

5 Discussion of the causality problem

In the sections above we have seen that, in contrast to the reflected field, the transmitted field is non-causal. This is, of course, highly non-physical, and, therefore, Condon's model must be discarded as a reliable model for bianisotropic media. However, we have also seen that, provided the parameter α is small in some sense, the violation of causality is limited. In this section we briefly discuss the range of validity of the model and the size of the parameter α obtained from experimental data.

As seen from Figures 2 and 3, the size of $\omega_0 \alpha c$ should be less than 10^{-2} m^{-1} to ensure that the effects of the non-causality are negligible. This result is under the assumption that the spatial variable ζ is of the order of or less than 1.

The typical size of the optical rotary power parameter α is given in Table 1, where the data is taken from [8]. From the table we see that the size of the constant α is in the range 10^{-20}–10^{-29} s^2/m. Moreover, we see that the range of the parameter $\omega_0 \alpha c$ is too large for most materials. Condon's model is, for these materials, not a good model for optical activity. However, for quarts at optical frequencies Condon's model is appropriate, despite the fact that the model is non-causal. The model might also be appropriate for the experiments made by Lindman early this century, but this depends on the value of the index of refraction, $\sqrt{\epsilon\mu}$, which is not available.

Material	κ	$\omega_0\alpha c$	$\omega_0/2\pi$	α
Quartz	$3.9 \cdot 10^{-5}$		$5.49 \cdot 10^{14}$	$3.77 \cdot 10^{-29}$
Lindman in 1914	0.05		$1.2 \cdot 10^{9}$	$2.12 \cdot 10^{-20}$
Metal helices in a resin matrix	0.44	0.27	$10 \cdot 10^{9}$	$2.34 \cdot 10^{-20}$
Metal helices in epoxy	1.78	0.34	$15 \cdot 10^{9}$	$6.3 \cdot 10^{-20}$
Copper strings in dielectric	0.16		$15 \cdot 10^{9}$	$5.66 \cdot 10^{-21}$
Ferroelectric ceramic strings	0.30	0.15	$8 \cdot 10^{9}$	$1.99 \cdot 10^{-20}$

Table 1: Data of the magnetoelectric parameter κ and the corresponding values of the parameters α and $\kappa/\sqrt{\epsilon\mu} = \omega_0\alpha c$ for a selection of materials at the frequency ω_0. The data is taken from [8].

Acknowledgment

Part of this work was performed during a Visiting Erskine Fellowship at the Department of Mathematics, University of Canterbury, Christchurch, New Zealand and this support is gratefully acknowledged.

A Solution to the boundary value problem

In this appendix all vectors and dyadics are two-dimensional depending on the spatial variable ζ and the time variable τ. The pertinent boundary value problem to be solved is

$$\begin{cases} \dfrac{\partial \boldsymbol{u}(\zeta,\tau)}{\partial \zeta} = \alpha \mathbf{J} \cdot \dfrac{\partial^2 \boldsymbol{u}}{\partial \tau^2}, & \zeta \geq 0 \qquad \tau \in \mathbb{R} \\ \boldsymbol{u}(0,\tau) = \boldsymbol{u}_0(\tau) \end{cases}$$

where $\boldsymbol{u}_0(\tau)$ given initial data.

We solve this boundary value problem by a Fourier transformation in time τ. The Fourier transform is defined as:

$$\begin{cases} \widehat{\boldsymbol{u}}(\zeta,\omega) = \displaystyle\int_{-\infty}^{\infty} \boldsymbol{u}(\zeta,\tau) e^{i\omega\tau}\, d\tau = \mathcal{F}(\boldsymbol{u}(\zeta,\cdot))(\omega) \\ \boldsymbol{u}(\zeta,\tau) = \dfrac{1}{2\pi} \displaystyle\int_{-\infty}^{\infty} \widehat{\boldsymbol{u}}(\zeta,\omega) e^{-i\omega\tau}\, d\omega = \mathcal{F}^{-1}(\widehat{\boldsymbol{u}}(\zeta,\cdot))(\tau) \end{cases}$$

The Fourier transform solution is

$$\widehat{\boldsymbol{u}}(\zeta,\omega) = e^{-\alpha\zeta\omega^2\mathbf{J}} \cdot \widehat{\boldsymbol{u}}_0(\omega) = \left\{ \mathbf{I}_2 \cos(\alpha\zeta\omega^2) - \mathbf{J} \sin(\alpha\zeta\omega^2) \right\} \cdot \widehat{\boldsymbol{u}}_0(\omega)$$

since $\exp \alpha\mathbf{J} = \mathbf{I}_2 \cos\alpha + \mathbf{J} \sin\alpha$.

The following inverse Fourier transforms are relevant ($a \in \mathbb{R}$):

$$\begin{cases} \mathcal{F}^{-1}(\hat{f}(\omega)\hat{g}(\omega))(\tau) = \displaystyle\int_{-\infty}^{\infty} f(\tau-\tau')g(\tau')\,d\tau' = (f*g)(\tau) \\ \mathcal{F}^{-1}(\cos a\omega^2)(\tau) = \dfrac{1}{\sqrt{4\pi|a|}}\cos\left(\tau^2/4|a| - \pi/4\right) \\ \mathcal{F}^{-1}(\sin a\omega^2)(\tau) = \dfrac{\operatorname{sign} a}{\sqrt{4\pi|a|}}\cos\left(\tau^2/4|a| + \pi/4\right) \end{cases}$$

Introduce the following dyadic-valued functions

$$\begin{cases} \mathbf{f}(a,\tau) = \dfrac{1}{\sqrt{4\pi|a|}}\cos\left(\tau^2/4|a| - \pi/4\right)\mathbf{I}_2 \\ \mathbf{g}(a,\tau) = -\dfrac{\operatorname{sign} a}{\sqrt{4\pi|a|}}\cos\left(\tau^2/4|a| + \pi/4\right)\mathbf{J} \end{cases}$$

The final solution is then

$$\boldsymbol{u}(\zeta,\tau) = \left(\mathbf{f}(\alpha\zeta,\cdot) * \boldsymbol{u}_0(\cdot)\right)(\tau) + \left(\mathbf{g}(\alpha\zeta,\cdot) * \boldsymbol{u}_0(\cdot)\right)(\tau) \tag{A.1}$$

where the temporal convolution of a dyadic-valued function $\mathbf{f}_1$ and a vector-valued function $\boldsymbol{f}_2$ is defined as

$$\left(\mathbf{f}(\zeta,\cdot) * \boldsymbol{g}(\cdot)\right)(\tau) = \int_{-\infty}^{\infty} \mathbf{f}(\zeta,\tau-\tau')\cdot\boldsymbol{g}(\tau')\,d\tau'$$

B Solution of the slab problem

In this appendix we solve the following nonstandard boundary value problem:

$$\begin{cases} \dfrac{d\boldsymbol{u}_\pm(z,t\pm z/c)}{dz} = \alpha\mathbf{J}\cdot\dfrac{\partial^2\boldsymbol{u}_\pm(z,t\pm z/c)}{\partial t^2}, & 0<z<L \\ \boldsymbol{u}_+(0^+,t) - r_0^-\boldsymbol{u}_-(0^+,t) = t_0^+\boldsymbol{E}_i(t) \\ r_L^+\boldsymbol{u}_+(L^-,t) - \boldsymbol{u}_-(L^-,t) = \mathbf{0} \end{cases} \qquad t\in\mathbb{R} \tag{B.1}$$

Note that the two fields $\boldsymbol{u}_\pm$ do not couple through the PDE, but they do couple through the boundary conditions.

The general solution to the PDE in the Fourier domain is, see Appendix A

$$\widehat{\boldsymbol{u}}_\pm(z,\omega) = e^{\pm i\omega z/c\mathbf{I}_2}e^{-\alpha z\omega^2\mathbf{J}}\cdot\widehat{\boldsymbol{u}}(0^+,\omega)$$

The boundary values imply

$$\begin{cases} \widehat{\boldsymbol{u}}_+(0^+,\omega) - r_0^-\widehat{\boldsymbol{u}}_-(0^+,\omega) = t_0^+\widehat{\boldsymbol{E}}_i(\omega) \\ r_L^+e^{i\omega L/c}\widehat{\boldsymbol{u}}_+(0^+,\omega) - e^{-i\omega L/c}\widehat{\boldsymbol{u}}_-(0^+,\omega) = \mathbf{0} \end{cases}$$

with solutions

$$\begin{cases} \widehat{\boldsymbol{u}}_+(0^+,\omega) = \dfrac{t_0^+}{1-r_0^- r_L^+ e^{2i\omega L/c}}\widehat{\boldsymbol{E}}_i(\omega) = t_0^+ \displaystyle\sum_{n=0}^{\infty} \big(r_0^-\big)^n \big(r_L^+\big)^n e^{2in\omega L/c}\widehat{\boldsymbol{E}}_i(\omega) \\ \widehat{\boldsymbol{u}}_-(0^+,\omega) = \dfrac{r_L^+ t_0^+ e^{2i\omega L/c}}{1-r_0^- r_L^+ e^{2i\omega L/c}}\widehat{\boldsymbol{E}}_i(\omega) = t_0^+ \displaystyle\sum_{n=0}^{\infty} \big(r_0^-\big)^n \big(r_L^+\big)^{n+1} e^{2i(n+1)\omega L/c}\widehat{\boldsymbol{E}}_i(\omega) \end{cases}$$

and the final solution to the finite slab problem is, see Appendix A

$$\begin{aligned} &\begin{pmatrix} \boldsymbol{u}_+(z,t) \\ \boldsymbol{u}_-(z,t) \end{pmatrix} \\ &\qquad = t_0^+ \sum_{n=0}^{\infty} \big(r_0^-\big)^n \big(r_L^+\big)^n \left[\mathbf{f}(\alpha z,\cdot) + \mathbf{g}(\alpha z,\cdot)\right] * \begin{pmatrix} \boldsymbol{E}_i(\cdot - z/c - 2nL/c) \\ r_L^+ \boldsymbol{E}_i(\cdot + z/c - 2(n+1)L/c) \end{pmatrix} \end{aligned} \tag{B.2}$$

C Fresnel Integrals

The Fresnel Integrals are defined as [1]:

$$\begin{cases} C(z) = \displaystyle\int_0^z \cos\Big(\frac{\pi}{2}t^2\Big)\,dt \\ S(z) = \displaystyle\int_0^z \sin\Big(\frac{\pi}{2}t^2\Big)\,dt \end{cases}$$

or expressed in the error function $\operatorname{erf}(z)$ as

$$C(z) + iS(z) = \frac{1+i}{2}\operatorname{erf}\left(\frac{\sqrt{\pi}}{2}(1-i)z\right)$$

Limiting values are

$$\begin{cases} \displaystyle\lim_{x\to\infty} C(x) = \frac{1}{2} \\ \displaystyle\lim_{x\to\infty} S(x) = \frac{1}{2} \end{cases}$$

which are easily found using the Cauchy integral on a segment ($0 < \arg z < \pi/4, 0 < |z| < \infty$) in the complex plane. Furthermore, the Fresnel integrals are odd in reflection in the origin,

$$\begin{cases} C(-z) = -C(z) \\ S(-z) = -S(z) \end{cases}$$

A useful integral is ($a > 0$) [1]

$$\int \sin\left(ax^2+2bx+c\right)\,dx = \sqrt{\frac{\pi}{2a}}\left\{\cos\left(\frac{b^2-ac}{a}\right)S\left[\sqrt{\frac{2}{a\pi}}(ax+b)\right] - \sin\left(\frac{b^2-ac}{a}\right)C\left[\sqrt{\frac{2}{a\pi}}(ax+b)\right]\right\}$$

From this integral it is easy to derive ($a > 0$)

$$\begin{aligned}\frac{1}{\sqrt{4\pi a}}\int_b^\infty &\cos\left((t-t')^2/4a \pm \pi/4\right)\sin\omega_0(t'-b)\,dt' \\ &= \sqrt{\frac{1}{8}}\{ -\cos\left(\omega_0(t-b)+\omega_0^2 a \mp \pi/4\right)[1/2+S(\gamma_+)] \\ &\quad +\sin\left(\omega_0(t-b)+\omega_0^2 a \mp \pi/4\right)[1/2+C(\gamma_+)] \\ &\quad +\cos\left(\omega_0(t-b)-\omega_0^2 a \pm \pi/4\right)[1/2+S(\gamma_-)] \\ &\quad +\sin\left(\omega_0(t-b)-\omega_0^2 a \pm \pi/4\right)[1/2+C(\gamma_-)]\}\end{aligned}$$

where $\gamma_\pm$ is

$$\gamma_\pm = \sqrt{\frac{8a}{\pi}}\left(\frac{t-b}{4a} \pm \frac{\omega_0}{2}\right)$$

From this expression it immediately follows that

$$\lim_{t\to-\infty}\frac{1}{\sqrt{4\pi a}}\int_b^\infty \cos\left((t-t')^2/4a \pm \pi/4\right)\sin\omega_0(t'-b)\,dt' = 0$$

We can also rewrite the expression as

$$\begin{aligned}\frac{1}{\sqrt{4\pi a}}\int_b^\infty &\cos\left((t-t')^2/4a \pm \pi/4\right)\sin\omega_0(t'-b)\,dt' \\ &= \frac{1}{4}\{ -\cos\left(\omega_0(t-b)+\omega_0^2 a\right)[1/2+S(\gamma_+)\pm 1/2 \pm C(\gamma_+)] \\ &\quad +\sin\left(\omega_0(t-b)+\omega_0^2 a\right)[1/2+C(\gamma_+)\mp 1/2 \mp S(\gamma_+)] \\ &\quad +\cos\left(\omega_0(t-b)-\omega_0^2 a\right)[1/2+S(\gamma_-)\pm 1/2 \pm C(\gamma_-)] \\ &\quad +\sin\left(\omega_0(t-b)-\omega_0^2 a\right)[1/2+C(\gamma_-)\mp 1/2 \mp S(\gamma_-)]\}\end{aligned}$$

from which we obtain the asymptotic behavior as $t \to \infty$

$$\begin{aligned}\frac{1}{\sqrt{4\pi a}}\int_b^\infty &\cos\left((t-t')^2/4a \pm \pi/4\right)\sin\omega_0(t'-b)\,dt' \\ &= \sin\omega_0(t-b)\begin{Bmatrix}\sin\omega_0^2 a \\ \cos\omega_0^2 a\end{Bmatrix} + f_\pm(t)\end{aligned} \tag{C.1}$$

where the function $f_\pm(t)$ is defined as

$$\begin{aligned} f_\pm(t) =& \frac{1}{4}\sin\omega_0(t-b)\left\{\left[\sin\omega_0^2 a \mp \cos\omega_0^2 a\right]\left[S(\gamma_+)+S(\gamma_-)-1\right]\right. \\ &\left. +\left[\cos\omega_0^2 a \pm \sin\omega_0^2 a\right]\left[C(\gamma_+)+C(\gamma_-)-1\right]\right\} \\ &+\frac{1}{4}\cos\omega_0(t-b)\left\{\left[\sin\omega_0^2 a \mp \cos\omega_0^2 a\right]\left[C(\gamma_+)-C(\gamma_-)\right]\right. \\ &\left. -\left[\cos\omega_0^2 a \pm \sin\omega_0^2 a\right]\left[S(\gamma_+)-S(\gamma_-)\right]\right\} \end{aligned}$$

and which vanishes as $t\to\infty$. The dominant asymptotic behavior is therefore

$$\begin{cases} \dfrac{1}{\sqrt{4\pi a}}\displaystyle\int_b^\infty \cos\left(\frac{(t-t')^2}{4a}+\frac{\pi}{4}\right)\sin\omega_0(t'-b)\,dt' \sim \sin\left(\omega_0(t-b)\right)\sin\omega_0^2 a \\ \dfrac{1}{\sqrt{4\pi a}}\displaystyle\int_b^\infty \cos\left(\frac{(t-t')^2}{4a}-\frac{\pi}{4}\right)\sin\omega_0(t'-b)\,dt' \sim \sin\left(\omega_0(t-b)\right)\cos\omega_0^2 a \end{cases}$$

as $t\to\infty$.

The limit values as $|t|\to\infty$ of the action of a function $f\in L_1(\mathbb{R})$ are also of interest. The following result is now proved ($a>0$):

$$\lim_{|t|\to\infty}\frac{1}{\sqrt{4\pi a}}\int_{\mathbb{R}}\cos\left((t-t')^2/4a\pm\pi/4\right)f(t')\,dt'=0,\quad f\in L_1(\mathbb{R}) \tag{C.2}$$

To see this the following limit is observed ($a>0$):

$$\int_a^b \cos\left(\alpha(t-t')^2\pm\pi/4\right)\,dt' = \frac{1}{\sqrt{2}}\int_{t-b}^{t-a}\left(\cos\alpha x^2\mp\sin\alpha x^2\right)\,dx\to 0,\ \text{as } |t|\to\infty$$

Now let $\phi(t)$ be a step function

$$\phi(t)=\sum_{k=1}^n \alpha_n\chi_{I_n}(t)$$

where I_n is an interval on the real line and $\chi_{I_n}(t)$ the characteristic function for the interval I_n. The result above implies that

$$\lim_{|t|\to\infty}\int_{\mathbb{R}}\cos\left((t-t')^2/4a\pm\pi/4\right)\phi(t')\,dt'=0$$

i.e.

$$\left|\int_{\mathbb{R}}\cos\left((t-t')^2/4a\pm\pi/4\right)\phi(t')\,dt'\right|\le\frac{\epsilon}{2},\qquad \text{for } |t|\ge T(\epsilon)$$

Now let $f\in L_1(\mathbb{R})$ and choose a sequence of step functions $\{\phi_n(t)\}_{n=1}^\infty$ such that [2]

$$\int_{\mathbb{R}}|f(t)-\phi_n(t)|\,dt\le\frac{\epsilon}{2},\qquad \text{for } n>N$$

for some N.

For all $\epsilon > 0$ the following estimate holds:

$$\begin{aligned}&\left|\int_{\mathbb{R}} \cos\left((t-t')^2/4a \pm \pi/4\right) f(t')\,dt'\right| \\ &\leq \int_{\mathbb{R}} |f(t') - \phi_n(t')|\,dt' + \left|\int_{\mathbb{R}} \cos\left((t-t')^2/4a \pm \pi/4\right) \phi_n(t')\,dt'\right| \\ &\leq \frac{\epsilon}{2} + \frac{\epsilon}{2} = \epsilon, \text{ for } |t| \geq T(\epsilon, n)\end{aligned}$$

for sufficiently large n.

D Delta sequences

Introduce the following notation:

$$\begin{cases} f(x) = \sqrt{\dfrac{2}{\pi}} \cos x^2 \\ g(x) = \sqrt{\dfrac{2}{\pi}} \sin x^2 \end{cases} \qquad \begin{cases} f_\alpha(x) = \dfrac{1}{\alpha} f(x/\alpha) \\ g_\alpha(x) = \dfrac{1}{\alpha} g(x/\alpha) \end{cases}$$

where $\alpha > 0$. The objective of this appendix is to prove that

$$\begin{cases} \lim\limits_{\alpha\to 0^+} f_\alpha(x) = \delta(x) \\ \lim\limits_{\alpha\to 0^+} g_\alpha(x) = \delta(x) \end{cases}$$

i.e.

$$\begin{cases} \lim\limits_{\alpha\to 0^+} \displaystyle\int_{-\infty}^{\infty} f_\alpha(x)\phi(x)\,dx = \phi(0) \\ \lim\limits_{\alpha\to 0^+} \displaystyle\int_{-\infty}^{\infty} g_\alpha(x)\phi(x)\,dx = \phi(0) \end{cases} \quad \text{for all } \phi \in C_0^\infty(\mathbb{R})$$

It is easy to verify that

$$\begin{cases} \displaystyle\int_{-\infty}^{\infty} f_\alpha(x)\,dx = \int_{-\infty}^{\infty} f(x)\,dx = 1 \\ \displaystyle\int_{-\infty}^{\infty} g_\alpha(x)\,dx = \int_{-\infty}^{\infty} g(x)\,dx = 1 \end{cases} \quad \text{for all } \alpha > 0$$

by using the limit values of the Fresnel Integrals $\lim_{x\to\infty} C(x) = \lim_{x\to\infty} S(x) = 1/2$, see also Appendix C. The following estimates are useful ($R > 0$):

$$\begin{cases} \left|\displaystyle\int_0^R f(x)\,dx - 1/2\right| \leq C_1/R \\ \left|\displaystyle\int_0^R g(x)\,dx - 1/2\right| \leq C_1/R \end{cases} \tag{D.1}$$

for some fixed constant C_1. These estimates are easily obtained by using the Cauchy integral on a segment $(0 < \arg z < \pi/4, 0 < |z| < R)$ in the complex plane.

We first address the limit of the function f_α and we define

$$r_\alpha(x) = \int_{-\infty}^{x} f_\alpha(x')\,dx' = \int_{-\infty}^{x/\alpha} f(x')\,dx'$$

and $|\, r_\alpha \,|_\infty \leq M$, where M is independent of α. For each $\alpha > 0$ the function $r_\alpha(x)$ is a continuous bounded function. Specifically, from (D.1) we have

$$\begin{cases} |r_\alpha(x)| \leq C_1/|x|, & x < 0 \\ |r_\alpha(x) - 1| \leq C_1/x, & x > 0 \end{cases} \tag{D.2}$$

This suggests that the corresponding distribution is the Heaviside function, *i.e.*

$$\lim_{\alpha\to 0^+} \int_{-\infty}^{\infty} r_\alpha(x)\phi(x)\,dx = \int_0^\infty \phi(x)\,dx \qquad \text{for all } \phi \in C_0^\infty(\mathbb{R})$$

We now prove this statement.

Assume that $\operatorname{supp}\phi \in [-R, R]$. For each $\epsilon > 0$ we have

$$\begin{aligned} \int_{-\infty}^{\infty} r_\alpha(x)\phi(x)\,dx = &\int_{-R}^{-\epsilon} r_\alpha(x)\phi(x)\,dx + \int_{-\epsilon}^{\epsilon} r_\alpha(x)\phi(x)\,dx \\ &+ \int_\epsilon^R (r_\alpha(x) - 1)\,\phi(x)\,dx + \int_\epsilon^\infty \phi(x)\,dx \end{aligned}$$

The following estimates holds, (use (D.2)):

$$\begin{cases} \displaystyle\int_{-R}^{-\epsilon} r_\alpha(x)\phi(x)\,dx \leq \|\phi\|_\infty C_1 \alpha \ln\frac{R}{\epsilon} \\ \displaystyle\int_\epsilon^R (r_\alpha(x) - 1)\,\phi(x)\,dx \leq \|\phi\|_\infty C_1 \alpha \ln\frac{R}{\epsilon} \end{cases}$$

and

$$\int_{-\epsilon}^{\epsilon} r_\alpha(x)\phi(x)\,dx \leq 2\epsilon\|\phi\|_\infty \|r_\alpha\|_\infty \leq 2\epsilon\|\phi\|_\infty M$$

Therefore, we have

$$\lim_{\alpha\to 0^+} \int_{-\infty}^{\infty} r_\alpha(x)\phi(x)\,dx = \lim_{\alpha\to 0^+} \int_{-\epsilon}^{\epsilon} r_\alpha(x)\phi(x)\,dx + \int_\epsilon^\infty \phi(x)\,dx$$

and in the limit $\epsilon \to 0$ we have, since $|\, r_\alpha \,|_\infty \leq M$ is independent of α

$$\lim_{\alpha\to 0^+} \int_{-\infty}^{\infty} r_\alpha(x)\phi(x)\,dx = \int_0^\infty \phi(x)\,dx$$

and we have proved that

$$\lim_{\alpha\to 0^+} r_\alpha(x) = H(x)$$

in the sense of distributions.

Furthermore, we have

$$r'_\alpha(x) = f_\alpha(x)$$

We get

$$\int_{-\infty}^{\infty} f_\alpha(x)\phi(x)\,dx = \int_{-\infty}^{\infty} r'_\alpha(x)\phi(x)\,dx = -\int_{-\infty}^{\infty} r_\alpha(x)\phi'(x)\,dx$$

Due to the fact that the distribution $\lim_{\alpha\to 0^+} r_\alpha = H$, and ϕ' is a test function, we get

$$\lim_{\alpha\to 0^+}\int_{-\infty}^{\infty} r_\alpha(x)\phi'(x)\,dx = \int_0^{\infty} \phi'(x)\,dx = -\phi(0)$$

and we obtain

$$\lim_{\alpha\to 0^+}\int_{-\infty}^{\infty} f_\alpha(x)\phi(x)\,dx = \phi(0) \qquad \text{for all } \phi\in C_0^\infty(\mathbb{R})$$

This proves that

$$\lim_{\alpha\to 0^+} f_\alpha(x) = \delta(x)$$

Similar analysis gives

$$\lim_{\alpha\to 0^+} g_\alpha(x) = \delta(x)$$

From the analysis above it is now easy to prove that

$$\begin{aligned}
&\lim_{a\to 0^+}\frac{1}{\sqrt{4\pi a}}\int_{-\infty}^{\infty}\cos\left(x^2/4a-\pi/4\right)\phi(x)\,dx\\
&=\lim_{\alpha\to 0^+}\frac{1}{\sqrt{\pi\alpha^2}}\int_{-\infty}^{\infty}\cos\left(x^2/\alpha^2-\pi/4\right)\phi(x)\,dx\\
&=\lim_{\alpha\to 0^+}\frac{1}{2}\int_{-\infty}^{\infty}\left(f_\alpha(x)+g_\alpha(x)\right)\phi(x)\,dx=\phi(0)
\end{aligned}$$

and

$$\begin{aligned}
&\lim_{a\to 0^+}\frac{1}{\sqrt{4\pi a}}\int_{-\infty}^{\infty}\cos\left(x^2/4a+\pi/4\right)\phi(x)\,dx\\
&=\lim_{\alpha\to 0^+}\frac{1}{\sqrt{\pi\alpha^2}}\int_{-\infty}^{\infty}\cos\left(x^2/\alpha^2+\pi/4\right)\phi(x)\,dx\\
&=\lim_{\alpha\to 0^+}\frac{1}{2}\int_{-\infty}^{\infty}\left(f_\alpha(x)-g_\alpha(x)\right)\phi(x)\,dx=0
\end{aligned}$$

for all $\phi \in C_0^\infty(\mathbb{R})$.

Thus

$$\begin{cases} \lim\limits_{a\to 0^+} \dfrac{1}{\sqrt{4\pi a}} \cos\left(x^2/4a - \pi/4\right) = \delta(x) \\ \lim\limits_{a\to 0^+} \dfrac{1}{\sqrt{4\pi a}} \cos\left(x^2/4a + \pi/4\right) = 0 \end{cases} \tag{D.3}$$

in the distributional sense.

References

[1] M. Abramowitz and I. A. Stegun, editors. *Handbook of Mathematical Functions*. Applied Mathematics Series No. 55. National Bureau of Standards, Washington D.C., 1970.

[2] H. S. Bear, editor. *A Primer of Lebesgue Integration*. Academic Press, San Diego, 1995.

[3] E. U. Condon. Theories of optical rotatory power. *Rev. Mod. Phys.*, **9**, 432–457, 1937.

[4] N. Engheta and D. L. Jaggard. Electromagnetic chirality and its applications. *IEEE Antennas and Propagation Society Newsletter*, pages 6–12, October 1988.

[5] A. Karlsson and G. Kristensson. Constitutive relations, dissipation and reciprocity for the Maxwell equations in the time domain. *J. Electro. Waves Applic.*, **6**(5/6), 537–551, 1992.

[6] A. Lakhtakia. Recent contributions to classical electromagnetic theory of chiral media: what next? *Speculations in Science and Technology*, **14**(1), 2–17, 1991.

[7] A. Lakhtakia, V. K. Varadan, and V. V. Varadan. *Time-Harmonic Electromagnetic Fields in Chiral Media*, volume 335 of *Lecture Notes in Physics*. Springer-Verlag, New York, 1989.

[8] I. V. Lindell, A. H. Sihvola, S. A. Tretyakov, and A. J. Viitanen. *Electromagnetic Waves in Chiral and Bi-isotropic Media*. Artech House, Boston, London, 1994.